FROM AERIAL IMAGES TO A DESCRIPTION OF REAL PROPERTIES

A Framework

Philipp Meixner and Franz Leberl

Institute for Computer Graphics and Vision, University of Technology, Inffeldgasse 16, 8010 Graz, Austria

Keywords: Aerial images, 3D-buildings, Image segmentation, Building floors, Window detection, Real property.

Abstract: We automate the characterization of real property and propose a processing framework for this task. Information is being extracted from aerial photography and various data products derived from that photography in the form of a true orthophoto, a dense digital surface model and digital terrain model, and a classification of land cover. To define a real property, one has available a map of cadastral property boundaries. Our goal is to develop a table for each property with descriptive numbers about the buildings, their dimensions, number of floors, number of windows, roof shapes, impervious surfaces, garages, sheds, vegetation, the presence of a basement floor etc.

1 REAL PROPERTIES

We define a "real property" by one or sometimes multiple parcels as they are recorded in cadastral maps. It consists of a piece of land, sometimes defined by a fence, on that land are one or more buildings, impervious surfaces, garages, trees and other vegetation. A property may also contain only the portion of a building, for example in dense urban cores where buildings are connected.

The description of a real property consists of a table with coordinates and other numbers. These define how many buildings exist, the type of building from a stored list of candidates, building height and footprint, number of floors, number and types of windows, presence of a basement floor, type of attic, roof type and roof details such as an eave, skylights, chimneys, presence of a garage and its size, types and extent of impervious surfaces such a driveway and parking spaces, and statements about the type and size of elements of vegetation, the presence of a water body, the existence and type of a fence etc.

A low cost solution seems feasible if one considers the wealth of aerial image source data currently being assembled for other applications, not insignificantly in connection with innovative location-aware Internet sites such as Google Maps, Microsoft Bing-Maps and others.

This paper presents a framework for processing steps that are necessary for a reasonable semantic interpretation and evaluation of real property using high resolution aerial images. Our initial focus is on characterizing individual properties and their buildings. This paper illustrates a set of work steps to arrive at a count of floors and windows.

2 LOCATION-AWARE INTERNET

2.1 Geodata for Location-Awareness

A location-aware Internet (Leberl, 2007) has evolved since about 2005. Internet-search has been a driving force in the rapid development of detailed 2-dimensional maps and also 3-dimensional urban models. "Internet maps" in this context consist of the street-maps used for car navigation, augmented by addresses, furthermore the terrain shape in the form of the Bald Earth and all this being accompanied by photographic texture from ortho photos. This is what is available for large areas of the industrialized World when calling up the websites maps.google.com or www.bing.com/maps, and in some form, this is also available under www.mapquest.com, maps.yahoo.com or maps.ask.com, as well as from a number of regional Internet mapping services.

Meixner P. and Leberl F. (2010).
FROM AERIAL IMAGES TO A DESCRIPTION OF REAL PROPERTIES - A Framework.
In *Proceedings of the International Conference on Computer Vision Theory and Applications*, pages 283-291
DOI: 10.5220/0002817602830291

Ubiquitous visibility of Geodata started with the development of car navigation systems for regular passenger cars. It signaled for the first time a transition from experts to everyone. The transition from being a tool for mere trip planning and address searches to true real-time navigation needed the GPS to become available, and that was the case since the mid 1990's.

"Urban Models" in 3D have been a topic of academic research since the early 1990's (Gruber, 1997). As part of Internet mapping, this came into being in November 2006 with Microsoft's announcement of the availability of Virtual Earth in 3D. The vertical man-made buildings are modeled as triangulated point clouds and get visually embellished by photographic texture. Since April 2008, vegetation is being classified and identified, and computer-generated vegetation is being placed on top of the Bald Earth.

Figure 1: Typical 3D content in support of an Internet search. Capitol in Denver (Microsoft's Bing-Maps).

The 3D urban models still are in their infancy and are provided over large areas only by the Microsoft-web site Bing/Maps, with an example presented in Figure 1. While Internet-search may be the most visible and also initial driving application, there of course are others. Often mentioned are city planning, virtual tourism, disaster preparedness, military or police training and decision making or car navigation.

2.2 Interpreted Urban Models

The 3D-data representing the so-called location awareness of the Internet serve to please the user's eye – one could speak of "eye candy" -- but cannot be used as part of the search itself. This is unlike the 2D content with its street map and address codes that can be searched. An interpreted urban 3D model would support searches in the geometry data, not just in the alphanumeric data. One may be interested in questions involving intelligent geometry data. Questions might address the number of buildings higher than 4 floors in a certain district, or properties with a built-up floor area in excess of 100 m2, with impervious areas in excess of 30% of the land area, or with a window surface in excess of a certain minimum.

Such requirements lead towards the interpretation of the image contents and represent a challenge for computer vision (Kluckner, Bischof, 2009).

While currently driven by "search", applications like Bing-Maps or Google Earth have a deeper justification in light of the emerging opportunities created by the Internet-of-Things and Ambient Intelligence. These have a need for location awareness (O'Reilly & Batelle, 2008).

3 A PROCESSING FRAMEWORK

We start out by conflating (merging) geometric data from two sources: the aerial imagery and the cadastral information. Figure 2 is an example for a 400 m x 400 m urban test area in the city of Graz (Austria). Conflation defines each property as a separate entity for further analysis. Conflation is part of a pre-processing workflow and results in all geometric data to be available per property and in a single geometric reference system.

We now proceed towards the use of the dense 3D point clouds associated with the aerial photography and extracted from it by means of a so-called dense matcher applied to the triangulated aerial photographs (Klaus, 2007). First is the extraction of data per building and per element of vegetation. This finds the areas occupied by a building as well as its height. For vegetation we need to find the type, its location, the height and the crown diameter. The building footprints get refined vis-à-vis the cadastral prediction using image segmentation and classification to define roof lines.

From the building one proceeds to the facades: building footprints become façade baselines. This footprint is the basis for an extraction of the façade in 3D by intersecting it with the elevation data. We compute the corner points of each façade. These can then be projected into the block of overlapping aerial photography. We can search in all aerial images for the best representation of the façade details; we prepare for a multi-view process.

What follows is a search for rows and columns of windows in the redundant photographic imagery. First of all, this serves to establish the number of floors. Second, we also are interested in the window locations themselves, as well as in their size. And finally, we want to take a look at attics and basement windows to understand whether there is an attic or basement.

Figure 3 summarizes the workflow towards a property characterization and represents the framework in which the effort is executed.

While an Internet application exists in the USA that associates with each property a value (www.zillow.com), this is based on public property tax records and no information is being extracted from imagery.

Figure 2: Left is a True Orthophoto of the city of Graz, 400 m * 400 m, at a ground sampling distance of 10 cm. Right is a cadastral map of Graz [Courtesy BEV-Austria].

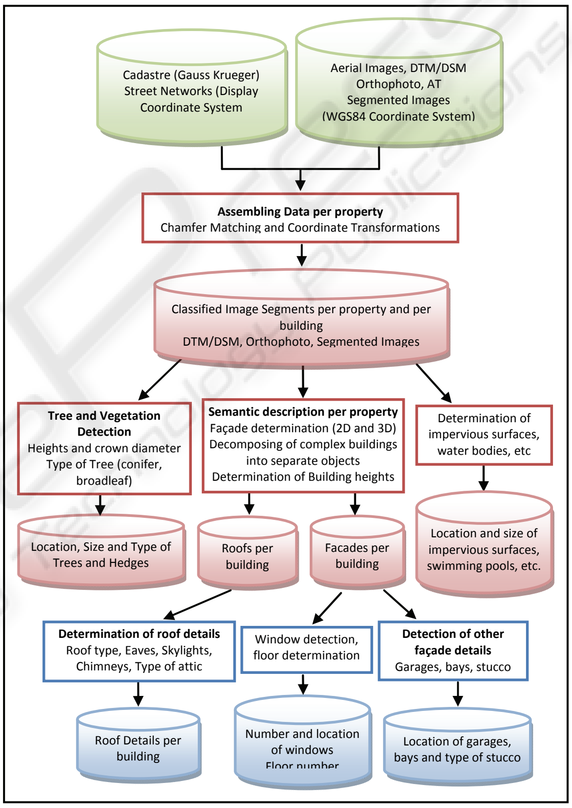

Figure 3: Diagram of the proposed work flow to characterize real properties from aerial images and associated cadastral data.

4 SOURCE DATA

4.1 Many Sources for Geo-Data

The diversity of geo-data is summarized in Table 1. It associates with each type of data source a geometric resolution or accuracy.

Table 1: The major sources of urban geo-data and their typical geometric resolution.

OVERHEAD SOURCE	URBAN GSD
1. Satellite Imagery	0.5 m
2. Aerial Imagery	0.1 m
3. Aerial Laser Scanning (LIDAR)	0.1 m
STREET SIDE SOURCES	
4. Street Side Imagery from Industrial Systems	0.02 m
5. Street Side Lasers	0.02 m
6. Crowd-Sourced Images (FLICKR, Photosynth)	0.02 m
7. Location Traces from Cell Phones and GNSS/GPS	5 m
OTHER DOCUMENTS	
8. Cadastral Maps, Parcel Maps	0.1 m
9. Street Maps from Car Navigation	5 m
10. Address codes with geographic coordinates (urban area)	15 m

The geometry of large urban areas is defined by aerial photography. While it may be feasible that a continuous future stream of perennially fresh GPS/GNSS-tagged collections of crowd-sourced imagery will do away with any need for aerial photography, that time has not yet arrived. A coordinate reference is thus being established by an automatically triangulated block of aerial photographs to within a fraction of a pixel across an entire urban space. Scholz and Gruber (2009) presented the triangulation results for the aerial images in the demo set to be within ± 0.5 pixels or ± 5 cm.

4.2 Aerial Images

In the current application, we process aerial images taken by the large format digital aerial camera UltraCam-X (Gruber et al., 2008). This, like most digital aerial cameras, produces images in the 4 colors red, green, blue and near infrared (NIR) and also collects a separate panchromatic channel. The images often have ~ 13 bits of radiometric range; this is encoded into 16 bits per color channel. The entire administrative area of the city of Graz consists of 155km² and covers the dense urban core and rural outlying areas. Of this surface area, a total of 3000 aerial photographs have been flown with an along-track overlap of 80% and an across-track overlap of

60%, and the Ground Sampling Distance GSD is at 10cm. It should be noted that this large number of aerial photographs far exceeds, by an order of magnitude, what one would have flown with a film camera for manual processing. The overlaps would have been at 60% and 20%, and the geometric GSD would have been selected at 20 cm, in order to keep the cost for film and for manual processing per film image at affordable levels.

Standard photogrammetric processing is being applied to such a block of digital photography using the UltraMap-AT processing system. Full automation is achieved first because of the high image overlaps; a second factor is the use of a very much larger number of tie-points than traditional approaches have been using.

4.3 DSM and DTM Data

The Digital Surface Model DSM is created by “dense matching”. The input consists of the triangulated aerial photographs. In the process, one develops point clouds from subsets of the overlapping images and then merges (fuses) the separately developed point clouds of a given area. The process is by Klaus (2007). The postings of the DSM and DTM are at 2 pixel intervals, thus far denser than traditional photogrammetry rules would support. The conversion of the surface model DSM into a Bald Earth Digital Terrain Model DTM is a post-process of the dense matching and has been described by Zebedin et al. (2006).

4.4 True Orthophoto

The DSM is the reference surface onto which each aerial photograph gets projected. The DSM and its associated photographic texture are then projected vertically into the XY-plane and result in what is denoted as a “true” orthophoto. In this data product, the buildings are only shown by their roofs, not, however by their facades. Given the overlaps of the source images, the orthophoto can get constructed such that all occlusions are being avoided. Image detail in the orthophoto is therefore taken from multiple aerial images in a manner that would not be customary in traditional film-based orthophotography.

4.5 Image Classification

Any urban area of interest is being covered by multiple color aerial images. These can be subjected to an automated classification to develop information layers about the area. We consider these to be an input into our characterization procedures. The classification approach used here has been described by Zebedin et al. (2006). However, classification and segmentation methods are topics of intense research. For example Kluckner, Bischof (2009) have proposed Random Forests as an alternative novel method with good results specifically interpreting urban scenes imaged by the UltraCam digital aerial camera.

Standard classifications of 4-channel digital aerial photography typically leads to 7 separate areas for buildings; grass; trees; sealed surfaces; bare Earth; water; other objects shown as “unclassified”. The unclassified areas may show lamp posts, cars, buses, people etc.

4.6 Cadaster

Since a “property boundary” is a legal concept, it is not typically visible in the field and from the air (Fig. 2 right). Also image segmentation algorithms cannot properly distinguish between buildings when they are physically attached to one another. It will be the rare exception that attached buildings can be separated from aerial imagery, for example if the roof styles differ, building heights vary or the colors of the roofing tiles differ. Obviously then, one needs to introduce the cadastral map.

Figure 4: Street layer from car navigation, also from Bing-Maps (left). Overlay with orthophoto (right), demo Graz.

The cadastral accuracy is being quoted at ± 15cm which is at the range of the aerial photography’s pixel size and thus sufficient for the purpose of characterizing real properties, in accordance with legislated standards.

4.7 Comments

Car navigation has been the driver for the global development of street maps. As a result, such data are available everywhere on the Internet. Figure 4 illustrates that the street layer does define properties against the public spaces, and can help in assessing the traffic issues for a given property.

All source data for the proposed property work are the result of extensive computation and data processing, some of it constituting the outcome of considerable and recent innovations, such as dense matching and fully automated triangulation. However, none of that processing is specific to the property characterization, and therefore is outside this application.

Much diversity has been and continues being developed in Geodata sources. There is considerable discussion about Google's involvement and its activities in driving along all roads, even rural ones, to develop not only a road network but all the associated addresses. Additionally, there is much talk about crowd sourced imagery, as typified by FLICKR, and about information contributed by users being denoted "neo-geographers".

5 DATA PER PROPERTY

5.1 Chamfer-Matching

Most cadastral maps, and so also the Austrian cadastre, basically present a 2D data base and ignore the 3rd dimension. This causes issues when relating the cadastral data to the aerial photography and its inherently 3D data products. In order to co-register two 2D data sets, an obvious approach is a match between the 2D-cadastral map with the 2D-orthophoto. Once this co-registration is achieved, the cadastral data are also geometrically aligned with all the other photo-derived data sets.

A 2-step process serves to match the cadastral map with its own coordinate system with the orthophoto in its different coordinate reference. In a first step, the cadastral point coordinates simply get converted from their Gauss-Krüger M34 values to the orthophoto's Universal Transverse Mercator UTM- system. In an ideal world, this would solve the registration problem. It does not. There exist small projection errors that can be seen in a segment in Figure 5 taken from the demonstration area. Local shifts in the range of a few pixels, thus some tens of centimeters, need to be considered.

5.2 Data per Property

The image classification result is in the same coordinate system as the orthophoto. Therefore the cadastral map can be used directly to cut a

Figure 5: Overlaying the cadastral map over the orthophoto will leave some small errors that need to be found and removed. Left after step1, right after step 2.

classification map into data per property. Figure 7 illustrates the result.

A second step is thus needed to achieve a fine alignment of the Cadastre and the Orthophoto. This adjustment is accomplished by a so-called Chamfer Match, here implemented after Borgefors (1988); Figure 6 illustrates the approach. Figure 5 shows discrepancies are reduced from their previous ± 7 pixels down to a mere ± 3 pixels.

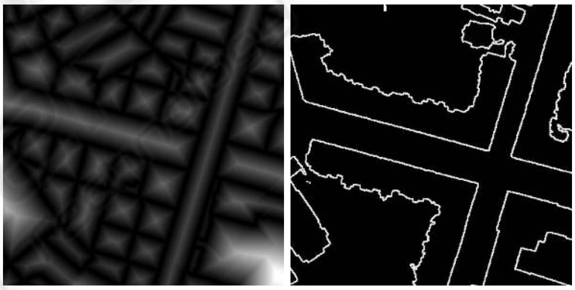

Figure 6: Cadastral raster distance image (left) and edge image (right) for a chamfer match.

Zebedin et al. (2006) deliver an accuracy of 90%. This is consistent with the current effort's conclusion. A source for discrepancies between cadastre and image is seen where the cadastral boundary line coincides with a building façade. One observes the existence of façade details such as balconies, or roof extensions in the form of eaves. Having the cadastre available offers one the option of changing the segmentation and classification.

5.3 Dense Point Clouds

In the current test area, the DSM/DTM are an elevation raster in the coordinate system of the photogrammetric block and at a posting interval of 20 cm. Cutting the large area dense DSM/DTM data set along property boundaries is trivial and based on the cadastral data after Chamfer refinement. Figure 7 contains an illustration of the result.

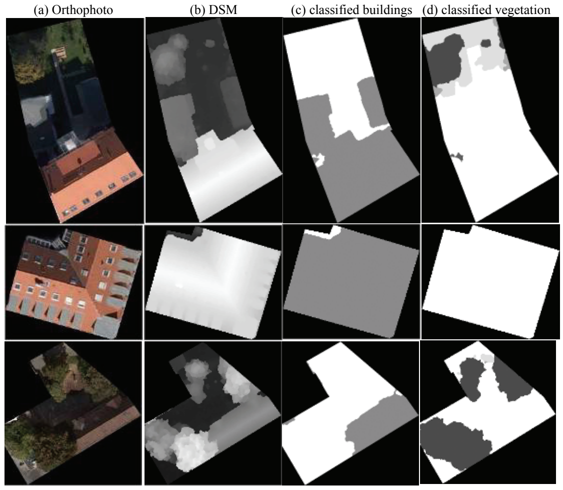

Figure 7: Three separate sample properties and the source data per property.

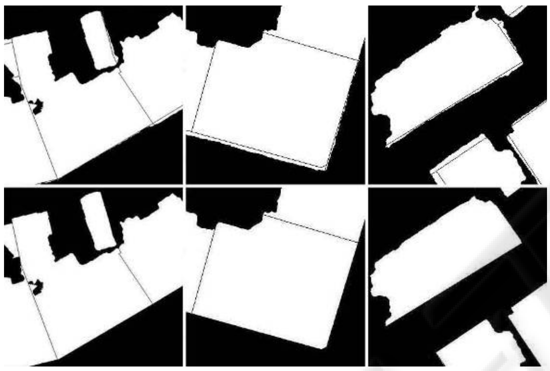

Figure 8: Overlay of segmented image and cadastre for areas in Figure 8. Above is with the discrepancies due to roof eaves and façade detail, below is a manually cleaned-up version.

6 PROPERTY DESCRIPTION

Several descriptions have become available as a byproduct of conflating the 2D cadastral data with the 2D imagery. We have not only defined the properties, but in the process we learned their land area, also the areas used up by the various object classes such as building, vegetation, water bodies or impervious surfaces. These measurements of surface area have previously been determined to be available at an accuracy of 90%.

However, we have yet to introduce into the work the 3rd dimension in the form of the dense point cloud. This will add the most relevant information

These considerations create the need for methods to automatically improve the alignment of the cadastral line work and the segmentation boundaries. Until such algorithms get developed and implemented, we perform such improvements by hand. Figure 8 illustrates the discrepancies and their removal.

The overriding role is associated with the buildings, and these are in the initial focus of the effort. All the work being applied is per property.

6.1 Facades Footprint 2D

Vectorizing the Building Contour. The building objects obtained from the image classification are an approximation of the intersection of a façade with the ground. One needs to isolate the contour of each building object in a given property. Initially, this contour is in the form of pixels in need of a vectorization. This is a well developed capability, one therefore has a choice of approaches. The Douglas-Peucker algorithm (Douglas, Peucker, 1973) is being used here. The goal is to replace the contour pixels by straight lines, each line defining a façade.

Vectorizing the Points along the Vertical Elements in the DSM. Separately, the 3D point cloud found for a building object also is a source for façades. Passing over the X-rows and Y-columns of the point cloud, one finds the building outline from the first derivative of the z-values – they represent the tangent to the point cloud and where this is vertical, a façade is present.

Reconciling the Segmentation Contour with the DSM Facade Points. The façade footprints from the image classification are based on color and texture and need to be reconciled with the footprint based on the 3D point cloud. One approach is to define the mean between the two largely independent measures.

A Property Boundary Cutting though two Connected Buildings. In the special case where a property boundary cuts through a building or a pair of connected buildings, one does not have a façade. Such cases need to be recognized. An approach is the use of the 3rd dimension, as shown below. The output of this step is a series of straight line segments representing multiple facades.

Decomposing a Building into Separate Building Objects. The option exists to fit into the pattern of façade footprints a series of predefined shapes of (rectangular) building footprints. In the process one hopes to develop a set of separate non-overlapping basic building objects. The 3rd dimension is being considered via roof shapes. Having more than one local maximum in the roof height is an indication that the single building should be segmented into multiple building objects.

6.2 Façades in the 3rd Dimension

Along the footprints of the façade one finds elevation values in the DSM. These do attach to the façade a 3rd dimension. Depending on the shape of the roof, a façade could have a complex shape as well. However, for use as a descriptor one might be satisfied with a single elevation value for each façade. We have now defined a vertical rectangle for each façade footprint.

A refinement would consist of a consideration of the change of elevations along the façade footprint. This could be indicative of a sloping ground, or of a varying roof line, or a combination of both. The slope of the ground is known from the DTM. The variations of the roof line are read off the difference between the DSM and the DTM.

The issue of connected buildings along a property line exists. One needs to identify such façade footprints since they are virtual only. Such facades can be identified via a look at the dense point cloud. The elevation values above the Bald Earth along a façade footprint will be zero at one side of the footprint. If they are not, then buildings are connected and this façade is only virtual.

6.3 Building and Roof Heights

A building has multiple façades (see Figure 9), and each façade represents a value for the height of the building. However, we have not yet considered the shape of the roof and therefore may get multiple building heights, depending on the façade one is considering. Two elevation numbers are desired to describe the building at a coarse level: we want to assign a single building height as well as a single roof height. The building height is the average of the façade heights. The roof height is the difference between the highest point in the building's point cloud that the previously computed building height.

6.4 Counting Floors and Windows

Conceptually we are dealing with a three-step process of analyzing each façade. First, we must project image content onto each façade rectangle or other façade shape. Therefore the corner points of a given façade get projected into each aerial photograph using the poses of the camera. That will define in each image a certain number of pixels. The image area with the highest number of pixels is likely to produce the best façade image. However, in the interest of using redundancy, we produce multiple façade images, one each per aerial photograph that exceeds a minimum image area to make sense in the further analysis.

Second, the image segments defined in this manner will have to be subjected to a floor count. An edge detector is applied to a given façade image and the edges are used for the floor count. Therefore the detected horizontal edge values will be transformed into a binary format and for each row a summation of the edge values will be performed. In a next step all the local maxima are detected and out of them the floors will be determined (see Figure 9).

Third is the definition of all the windows. This task has recently received some attention, for example by Čech and Šára (2007). The window detection uses the normalized horizontal as well as vertical gradients. Our approach is taken from Lee and Nevatia (2004). It extracts windows automatically via a profile projection method from each of the single façade images. The Prewitt edges get projected along the rows and columns of the façade image and the accumulations of the edges signify the presence or absence of a window row or window column. We define straight lines along the boundary of each accumulation, thereby obtaining likely candidates for window areas in the 2D plane of the façade. This method is not very accurate when there are different shapes of windows in the same column or line. To refine the window locations a one dimensional search for the four sides of a window is performed. Hypothesized lines are generated by moving the line to its perpendicular direction and test them. The refined position of the window is where the hypothesized line has the best score for the window boundary. Details are available from Lee and Nevatia (2004).

Figure 10 illustrates the result for the example of one façade, yet multiple images, and indicates that the window areas do get defined to within ± 3 pixel in both the horizontal as well as vertical dimensions, converting to a value of ± 0.3 m vertically and ± 0.3 m horizontally. In the example shown in Figure 11, all 33 windows of the façade were found in all 4 aerial images. As one can see in Figure 10 also the 6 basement window openings in every façade could be detected by evaluating their positions and size in the image. A door is also detected using its size and location.

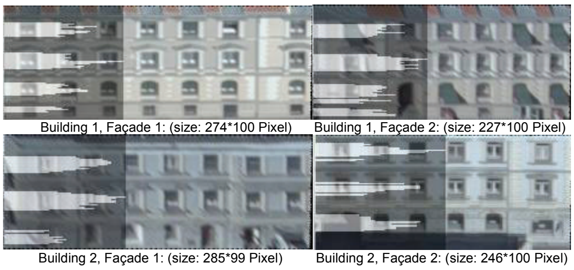

Figure 9: One single building has multiple façades.

6.5 Discussion

The approach produces key numbers per building We also obtain a measure of consistency (a) from multiple façades for one and the same building and (b) between the results from multiple overlapping images (Figure 10). The approach also delivers the basis for further detail such as shapes and types of windows, separating façade openings into windows and doors, defining attic and basement floors. These key numbers are based on 3D-data about a property and on the original aerial images showing façade detail.

Initial work indicates that for some sample properties like those shown in Figure 7, all floors and all windows have been found automatically in each façade, delivering a rather robust result.

Much, however, remains to be done to obtain a good understanding of the accuracy and reliability of these key numbers, the problems one will have when parts of a building are occluded, when the geometric resolution of the source data varies, when buildings deviate from a standard shape in the event of add-ons, have complex footprints and roof shapes, when cadastral detail contradicts image detail etc.

7 CONCLUSIONS

It is the main purpose of this paper to introduce an application of vast 3D urban Geodata bases to automatically characterize real properties. This may be of value in managing location-based decisions both in commercial and public interest environments, and to better administrate municipal resources. This task is made feasible by the rapid increase in urban 2D- ad 3D-data which in turn are being produced in growing quantities for new applications of the Internet. Global Internet search providers like Google, Microsoft, Yahoo and Ask all have developed a mapping infrastructure for location-aware search systems. They have embarked on significant efforts to conflate various 2D Geodata

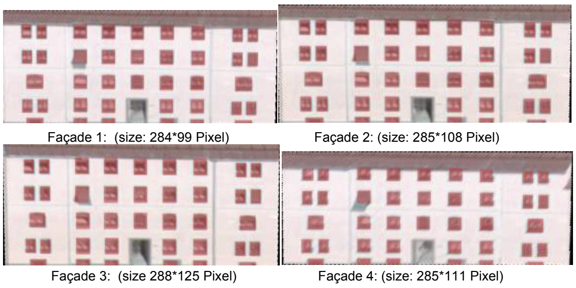

Figure 10: One single façade of one single building is shown four times in overlapping images.

sources, to add business and private address data bases, parcel data, GNSS and cellular traces and have started to add the 3rd dimension, both from aerial as well as street-side images. It is the latter that is expected to be contributed largely from user-generated content (UGC). While the initial battleground for Google and Microsoft is in the search application, one can already see on the horizon spatial information as an integral part of the evolution of the Internet-of-Things ("IoT") and of Ambient Intelligence ("AmI").

To actually succeed in the automated property description, one will use the original overlapping aerial images and Geodata derived from the aerial material. This derived material is in the form of orthophotos, digital elevation models and pose information for each aerial photograph. The proposal presented for an end-to-end property characterization adds to these data the cadastral parcel information, and potentially the existing street maps.

Obviously, one can expect the ease and accuracy of the data extracted for a property to be a function of the quality of the source material, in particular of the elevation data and geometric resolution of the aerial imagery. While the study of the influence of source data quality will be a topic for ongoing work, we already have developed indications that counting floors and windows poses fairly relaxed demands on the image quality and pixel size. Initial sample data on but a few, yet typical properties in an urban core indicate that all floors and all windows could be counted correctly.

ACKNOWLEDGEMENTS

Aerial images, DSM, True Orthophotos and segmented images were provided by Vexcel Imaging Graz (Microsoft). Help is greatly appreciated, as provided by B. Gruber, M. Gruber

(Microsoft), and by M. Donoser, S. Kluckner and G. Pacher (ICG-TU Graz).

REFERENCES

Borgefors G, 1988: Hierarchical chamfer matching: a parametric edge matching algorithm, *IEEE trans. Pattern Analysis Machine Intelligence*, vol. 10, no. 6, pp. 849–865.

Čech J., R. Šára (2007) *Windowpane detection based on maximum aposteriori labeling.* Technical Report TR-CMP-2007-10, Center for Machine Perception, K13133 FEE Czech Technical University, Prague.

Douglas D., T. Peucker (1973), Algorithms for the reduction of the number of points required to represent a digitized line or its caricature, *The Canadian Cartographer* pp. 112-122.

Gruber M.(1997) *Ein System zur umfassenden Erstellung und Nutzung dreidimensionaler Stadtmodelle*, Dissertation, Graz Univ. of Technology, 1997.

Gruber M., M. Ponticelli, S. Bernögger, F. Leberl (2008) UltracamX, the Large Format Digital Aerial Camera System by Vexcel Imaging / Microsoft. *Proceedings of the Intl. Congress on Photogrammetry and Remote Sensing*, Beijing, July 2008

Klaus A. (2007) Object Reconstruction from Image Sequences. Dissertation, Graz Univ. of Technology, 1997.

Kluckner S., H. Bischof (2009) Semantic Classification by Covariance Descriptors within a Randomized Forest. *Proceedings of the IEEE International Conference on Computer Vision, Workshop on 3D Representation for Recognition* (3dRR-09)

Leberl F. (2007) Die automatische Photogrammtrie für das Microsoft Virtual Earth *Internationale Geodätische Woche Obergurgl*. Chesi/Weinold (Hrsg.), Wichmann-Heidelberg-Publishers, pp. 200-208

Lee S.C., R. Nevatia (2004) Extraction and Integration of Window in a 3D Building Model from Ground View Images. *Proc. IEEE Computer Society Conference on Computer Vision and Pattern Recognition CVP'04*

O'Reilly T., J. Batelle (2009) *Web Squared: Web 2.0 Five Years On*. O'Reilly Media Inc. Available from www.web2summit.com.

Scholz S., M. Gruber (2009) Radiometric and Geometric Quality Aspects of the Large Format Aerial Camera UltraCam Xp. *Proceedings of the ISPRS*, Hannover *Workshop 2009 on High-Resolution Earth Imaging for Geospatial Information*, XXXVIII-1-4-7/W5, ISSN 1682-1777

Zebedin L., A. Klaus, B. Gruber-Geymayer, K. Karner (2006) Towards 3D map generation from digital aerial images. *ISPRS Journal of Photogrammetry and Remote Sensing,* Volume 60, Issue 6, September 2006, Pages 413-427